



HAL
open science

Stiffness mapping of metastatic pelvic bone

Cléa Sieffert, Laurence Meylheuc, Bernard Bayle, Julien Garnon

► **To cite this version:**

Cléa Sieffert, Laurence Meylheuc, Bernard Bayle, Julien Garnon. Stiffness mapping of metastatic pelvic bone. 2024. hal-04738032

HAL Id: hal-04738032

<https://hal.science/hal-04738032v1>

Preprint submitted on 15 Oct 2024

HAL is a multi-disciplinary open access archive for the deposit and dissemination of scientific research documents, whether they are published or not. The documents may come from teaching and research institutions in France or abroad, or from public or private research centers.

L'archive ouverte pluridisciplinaire **HAL**, est destinée au dépôt et à la diffusion de documents scientifiques de niveau recherche, publiés ou non, émanant des établissements d'enseignement et de recherche français ou étrangers, des laboratoires publics ou privés.



Distributed under a Creative Commons Attribution 4.0 International License

Stiffness mapping of metastatic pelvic bone

Cléa Sieffert *

ICube UMR 7357 Strasbourg University - CNRS,
Strasbourg, France

Laurence Meylheuc

ICube UMR 7357 Strasbourg University - CNRS,
Strasbourg, France & INSA Strasbourg, Strasbourg,
France

Bernard Bayle

ICube UMR 7357 Strasbourg University - CNRS,
Strasbourg, France

Julien Garnon

ICube UMR 7357 Strasbourg University - CNRS,
Strasbourg, France & Strasbourg University
Hospital, Strasbourg, France

*Corresponding author. Email: clea.sieffert@insa-strasbourg.fr

Keywords: Cementoplasty; Oncology; Bone metastasis; Material mapping.

1. Introduction

Cementoplasty is a minimally invasive procedure used for the treatment of patients with bone metastases. When combined with screws, it is effective in consolidating pathologic fractures and treating associated pelvic pain (Deschamps et al. 2018). However, adequate placement of screws and determination of the optimal cement amount for each patient remain a burning issue (Garnon et al. 2019). Numerical finite element models developed from intra-operative images of patients are a first-rate way to explore different screw placements and cement volumes to answer these questions. Before simulating the best mechanical restoration strategy of the pelvis with cementoplasty, an accurate bone stiffness model of the diseased pelvis must be first developed. Commonly used bone models typically consist of two distinct parts: the thin superficial cortical zone and the inner trabecular zone. In addition, there are several ways to model metastases using the finite element method in the literature. They are often simply modeled in the pelvis by empty cavities (Morris et al. 2022; Li et al. 2006). A more accurate approach is to determine their local stiffness from pre-operative CT scan images, as shown for femoral shafts by Keyak et al. (2005). The objective of this work is to extend this

approach to model the local stiffness of the pelvic bone, including metastatic regions based on CT images of patients. Particularly, the local stiffness distribution between healthy and diseased iliac wing is compared.

2. Methods

A patient with a pathologic fracture caused by a large metastasis of 135 ml (33% of the total volume of his left wing) is selected for the study. From pre-operative CT scans of the pelvis, the surfaces of both healthy and diseased iliac wings are manually segmented with a slicer tool (voxel size 1x1x0.3mm). Solid 3D models are then reconstructed from the segmented surfaces using CAD software to obtain tetrahedral meshes of the wings. These two meshes are then exported to the mechanical property mapping software BoneMat. The formulae for correlating bone density to ash-density (1) and the equation between ash-density and the Young's modulus (2) are based on the study by Schileo et al. (2014):

$$(1) \rho_{Ash} = 0.877\rho_{QCT} + 0.079$$

$$(2) E = 14664\rho_{Ash}^{1.49}$$

The resulting mapped meshes of the bone are then processed to study its distribution. The Young's modulus associated to each mesh element is extracted from BoneMat generic mesh files. To compare the healthy iliac wing results with the literature, the minimum, maximum and median apparent densities are computed using the following relationship between ash and apparent density: $\rho_{Ash} = 0.6\rho_{app}$ (Schileo et al. 2014). Finally, for healthy and diseased modulus distribution comparison, the number of elements with a Young's modulus in MPa included in the following three intervals are computed: soft [0; 700], semi-rigid [700; 3000] and rigid bone [3000; 15000].

3. Results and discussion

Table 1. Distribution of Young's modulus over the wings. Credit: Cléa Sieffert

E [MPa]	[0;700]	[700;3000]	[3000;15000]
Healthy wing	16%	46%	38%
Diseased wing	32%	37%	31%

The apparent density value for the healthy wing averaged 0.45 g/cm³ with a maximum of 1.6 g/cm³ and a minimum of 0.08 g/cm³. These results are slightly higher than those obtained by Dalstra et al (1993). This discrepancy can be explained by the fact that they studied only the trabecular bone of the iliac wing, whereas we mapped the entire wing, including the cortical bone which has a higher density than the trabecular bone.

The comparison of the modulus distribution in Table 1 between the healthy and diseased wings outlines a 16% increase in the number of elements with a Young's

modulus within the 0-700 MPa range. These distribution variations also affect the value of the median modulus, which decreases by 35% (2084 MPa for the healthy wing compared to 1357 MPa for the diseased wing). However, extreme values remain similar, with a maximum about 14000 MPa and a minimum of 334 MPa for both cases. Figure 1 illustrates the metastatic effect, with an extended region with low moduli in the left wing, mainly due to the cortical deterioration caused by the disease. Such damages will have direct consequences on the mechanical strength of the pelvis by creating weakness areas during load transfers while walking.

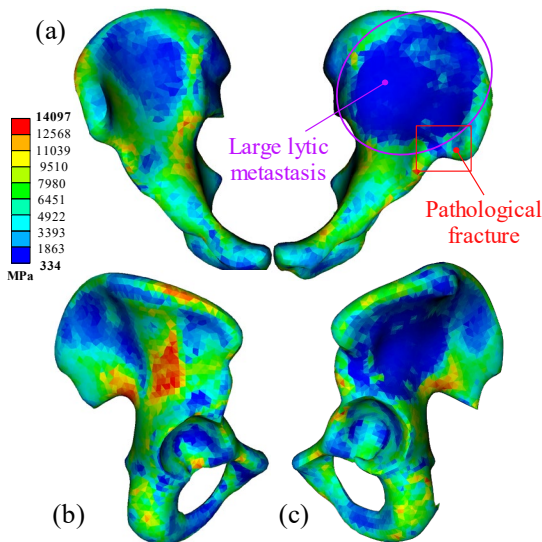


Figure 1. Mapping of the Young's modulus over the healthy and diseased iliac wing. (a) Front view of the pelvis; (b) side view of the right healthy wing; (c) side view of the left diseased wing. Credit: Cléa Sieffert

4. Conclusion

The mapping of mechanical properties based on the patient's CT scan highlighted the effect of the metastases on the local distribution of bone stiffness. The next steps will be to study the impact of these local variations on the global stiffness by implementing finite element models of both wings. Different scenarios with different amounts of cement and screw placement will then be assessed to determine the best combination to restore the patient's original pelvic stiffness.

Funding

This work of the Interdisciplinary Thematic Institute HealthTech, as part of the ITI 2021-2028 program of the University of Strasbourg, CNRS and Inserm, was supported by IdEx Unistra and SFRI under the framework of the French Investments for the Future Program.

Conflict of Interest Statement

The authors have no relevant conflicts of interest to disclose.

References

- Dalstra M, Huiskes R, Odgaard A, van Erning L. 1993. Mechanical and textural properties of pelvic trabecular bone. *Journal of Biomechanics*. 26(4):523–535. doi:10.1016/0021-9290(93)90014-6
- Deschamps F, Yevich S, Gravel G, Roux C, Hakime A, Baère T de, Tselikas L. 2018. Percutaneous Fixation by Internal Cemented Screw for the Treatment of Unstable Osseous Disease in Cancer Patients. *Semin Intervent Radiol*. 35(04):238–247. doi: 10.1055/s-0038-1673359
- Garnon J, Meylheuc L, Cazzato RL, Dalili D, Koch G, Auloge P, Bayle B, Gangi A. 2019. Percutaneous extra-spinal cementoplasty in patients with cancer: A systematic review of procedural details and clinical outcomes. *Diagnostic and Interventional Imaging*. 100(12):743–752. doi: 10.1016/j.diii.2019.07.005
- Keyak JH, Kaneko TS, Rossi SA, Pejic MR, Tehranzadeh J, Skinner HB. 2005. Predicting the Strength of Femoral Shafts with and without Metastatic Lesions. *Clinical Orthopaedics and Related Research*. doi: 10.1097/01.blo.0000174736.50964.3b
- Li Z, Butala NB, Etheridge BS, Siegel HJ, Lemons JE, Eberhardt AW. 2006. A Biomechanical Study of Periacetabular Defects and Cement Filling. *Journal of Biomechanical Engineering*. 129(2):129–136. doi: 10.1115/1.2472367
- Morris MT, Alder KD, Moushey A, Munger AM, Milligan K, Toombs C, Conway D, Lee I, Chen F, Tommasini SM, Lee FY. 2022. Biomechanical restoration of metastatic cancer-induced periacetabular bone defects by ablation-osteoplasty-reinforcement-internal fixation technique (AORIF): To screw or not to screw? *Clinical Biomechanics*. 92: 105565. doi: 10.1016/j.clinbiomech.2021.105565
- Schileo E, Balistreri L, Grassi L, Cristofolini L, Taddei F. 2014. To what extent can linear finite element models of human femora predict failure under stance and fall loading configurations? *Journal of Biomechanics*. 47(14):3531–3538. doi: 10.1016/j.jbiomech.2014.08.024

Received date:05/04/2024

Accepted date: 28/06/2024

Published date: XX/XX/2024

Volume: 1

Publication year: 2024